

# Flexible-format Optical Modulators with a Hybrid Configuration of Silica Planar Lightwave Circuits and LiNbO<sub>3</sub> Phase Modulators

*Hiroshi Yamazaki<sup>†</sup> and Takashi Goh*

### Abstract

We have devised and fabricated two types of flexible-format optical modulators that let us flexibly change the modulation format: a single-carrier modulator, which supports 4-, 8-, and 16-level modulations, and a multicarrier modulator, which provides a selectable combination of the number of frequency carriers and modulation levels. Both were fabricated using a hybrid integration of silica planar lightwave circuits and LiNbO<sub>3</sub> phase modulators and successfully operated at high baud rates corresponding to >100 Gbit/s. These technologies are promising for future spectrally efficient optical networks in which various modulation formats are used flexibly and adaptively.

### 1. Introduction

Multilevel modulation formats, such as N-level phase-shift keying (N-PSK) and N-level quadrature amplitude modulation (N-QAM), are the keys to achieving a large transmission capacity and high spectral efficiency (SE) in wavelength-division multiplexed (WDM) optical transmission systems. A record transmission capacity of 69.1 Tbit/s with SE of 6.4 bit/s/Hz has been achieved using polarization-division-multiplexed (PDM) 16QAM [1]. However, a higher modulation level, which offers higher SE, also leads to lower receiver sensitivity, which means a shorter transmission distance [2]. Because of this trade-off, the choice of modulation level may vary with the system design, so a transmitter that supports multiple modulation formats will be useful. Furthermore, flexible switching of modulation formats in response to optical path switching will be beneficial for maintaining the maximum SE for each channel in future all-optical networks (also called transparent

networks) in which signals are switched without optical-to-electrical and electrical-to-optical conversion [3].

To generate multilevel optical signals, multilevel electronics, such as arbitrary waveform generators or digital-to-analog converters, have been used in many transmission experiments [3]–[5]. With such multilevel electronics, we can cover various modulation formats with a simple optical setup. On the other hand, optical multilevel-signal syntheses, in which only binary electronics are used, have also been studied extensively [1], [2], [6]–[10]. Those schemes are promising for high-speed multilevel modulations because binary electronics pose fewer challenges for high-speed operation than multilevel electronics do [6], [7]. However, they have lacked flexibility; different optical configurations have been required for different modulation formats.

In this study, we devised two types of flexible-format optical modulator using optical multilevel-signal syntheses. One is a single-carrier flexible-format modulator, which supports 4-, 8-, and 16-level modulation formats [11]. The other is a multicarrier flexible-format modulator, which provides frequency-division-multiplexed (FDM) multilevel modulation

<sup>†</sup> NTT Photonics Laboratories  
Atsugi-shi, 243-0198 Japan

with a selectable combination of the number of frequency carriers and modulation levels [12]. Both modulators let us change the SE at the cost of a reduced transmission distance without changing the baud rate. The main difference is that the single-carrier type changes the bit rate and keeps the spectral bandwidth, while the multicarrier type changes the spectral bandwidth and keeps the bit rate. We fabricated them using a hybrid integration of silica planar lightwave circuits (PLCs) and LiNbO<sub>3</sub> (LN) phase modulators, which is promising for fabricating advanced multilevel modulators with both a large electro-optic bandwidth and complicated optical configurations [10]–[13]. The modulators successfully operated at high baud rates corresponding to bit rates of >100 Gbit/s.

## 2. Single-carrier flexible-format modulator

### 2.1. Design and fabrication

The single-carrier modulator was designed to support quadrature-PSK (QPSK), 8PSK, 8QAM, and 16QAM. These  $2^N$ -level signals ( $N=2, 3, 3,$  and  $4$ , respectively) can be generated through optical signal syntheses using  $N$  binary-driven Mach-Zehnder modulators (MZMs) [6]. We designed the modulator so that it has four MZMs and tunable circuits with which we can select the number of MZMs contributing to the modulation.

The optical-circuit configuration of the modulator is shown in **Fig. 1**. It has a two-stage lattice configuration. In the first stage, each arm has an MZM. In the second stage, the upper arm has two MZMs connected in parallel plus a pair of tunable couplers while the lower arm does not have any functional components. The couplers at the input of the first stage and between the first and second stages are static 3-dB couplers, while the one at the output of the second stage is another tunable coupler. The four MZMs (denoted MZMs 1–4) are driven in push-pull conditions with different binary data signals, Data 1–4, respectively. All data signals have an amplitude of  $2V\pi$ , so the MZMs operate as binary-PSK (BPSK) modulators. MZMs 2 and 4 are followed by  $\pi/2$  phase shifters. The power coupling ratios of the tunable couplers,  $\alpha:1-\alpha$  and  $\beta:1-\beta$  (upper to lower arms), as denoted in the figure, are varied for different modulation formats. The relative optical phase between the upper and lower arms of the second stage,  $\phi$ , is also varied.

The operating principle is as follows. The signal constellations at points A, B, and C and at the final

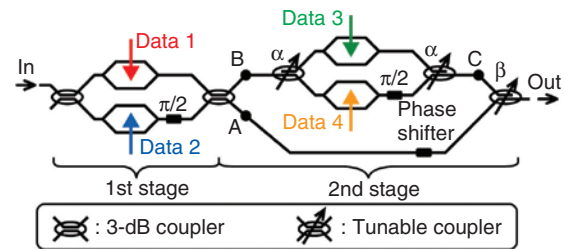


Fig. 1. Optical-circuit diagram of the single-carrier flexible-format modulator.

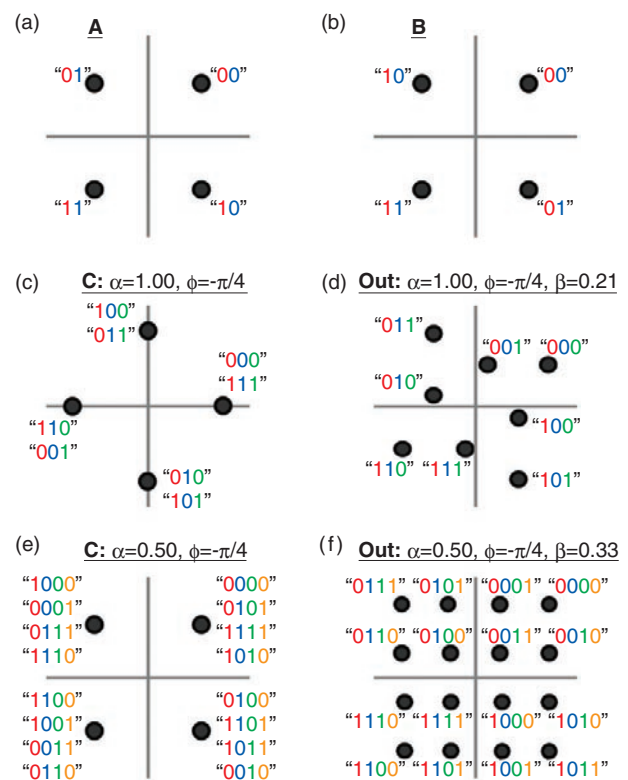


Fig. 2. Schematic constellations and data mappings at A, B, C, and Out in Fig. 1.

output port are shown in **Fig. 2**. Here, the data values 1 and 0 are allocated to optical phases 0 and  $\pi$ , respectively, in each BPSK signal generated with an MZM. A binary data string at each signal point (e.g., 1100) represents the values of Data 1–4 from left to right. As shown in Figs. 2(a) and (b), the first stage sends two QPSK signals to the two arms of the second stage. Those two signals have the same amplitudes but different (mirror-symmetric) data mappings. By setting  $\beta=0$ , we can obtain the QPSK signal

shown in Fig. 2(a) as the modulator's final output. An 8QAM signal is generated when  $\alpha=1$ ,  $\varphi=-\pi/4$ , and  $\beta=1/(3+\sqrt{3})\approx 0.21$ . In this case, MZM 3 converts the QPSK signal shown in Fig. 2(b) into the signal shown in Fig. 2(c), in which eight values of 3-bit data degenerate to four signal points. This double degeneracy is broken when the signals from the upper and lower arms (Figs. 2(c) and (a)) are coupled, and the modulator outputs the 8QAM signal shown in Fig. 2(d). An 8PSK signal can also be generated in the same manner with  $\alpha=1$ ,  $\varphi=-\pi/2$ , and  $\beta=\tan^2(\pi/8)/(1+\tan^2(\pi/8))\approx 0.15$ . To obtain a 16QAM signal, we set  $\alpha=0.5$ ,  $\varphi=-\pi/4$ , and  $\beta=1/3\approx 0.33$ . With this condition, the upper-arm signal has quadruple degeneracy (Fig. 2(e)), which is broken by the coupling with the lower-arm signal (Fig. 2(a)). The final output is the 16QAM signal shown in Fig. 2(f). As described above, we can flexibly switch the modulation level simply by using tunable couplers and a phase shifter. Furthermore, with the lattice configuration, the modulation losses for 8- and 16-level modulations are smaller than those with previously reported schemes [11].

We fabricated the modulator with the configuration shown in Fig. 3. We used two PLCs (PLC-L and -R) and an X-cut LN chip and implemented the modulator circuit with a compact loop-back configuration. The LN chip has an array of eight straight phase modulators, four signal electrodes (coplanar waveguides), and a passive straight waveguide. The PLCs contain all other circuit components: Y-branches for MZMs, 3-dB wavelength-insensitive couplers (WINC), tunable couplers, and U-turn waveguides. Each tunable coupler consists of Mach-Zehnder circuits with a thermo-optic phase shifter in each arm. We bonded the chips to each other with ultraviolet-curable (UV-curable) adhesive and then mounted them on an SUS package with radio-frequency connectors. The PLC-L, LN, and PLC-R chips are 29.0 mm  $\times$  6.5 mm, 64.0 mm  $\times$  6.0 mm, and 17.0 mm  $\times$  6.5 mm, respectively, giving a total chip length of 110 mm.

## 2.2. Characteristics

At a wavelength of 1550 nm, the insertion loss of the modulator with  $\beta=0$  is 7.3 dB and that with  $\beta=1$  and  $\alpha=0.5$  is 7.5 dB. The difference of 0.2 dB corresponds to the excess loss in MZMs 3 and 4 and in the two tunable couplers. The 3-dB bandwidths of the electro-optic frequency responses are around 25 GHz for all MZMs.

We tested the modulator in the single-polarization back-to-back setup shown in Fig. 4. The light source

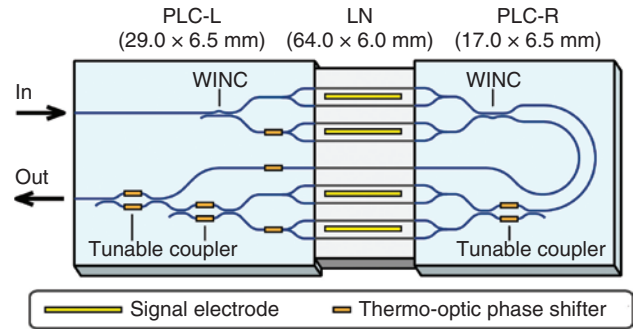


Fig. 3. Configuration of the single-carrier flexible-format modulator.

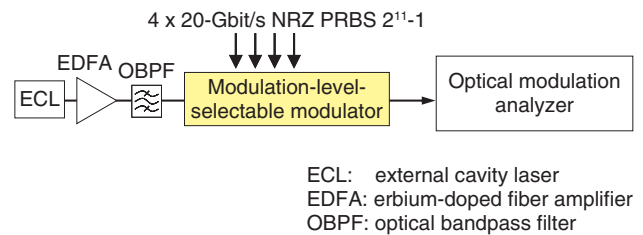


Fig. 4. Experimental setup.

was an external-cavity laser with a wavelength of 1551 nm and linewidth of  $\sim 30$  kHz. The modulator was driven with four 20-Gbit/s non-return-to-zero (NRZ)  $2^{11}-1$  pseudo-random bit sequences (PRBSs) with different delays. We switched the modulation formats by using the tunable couplers as described above, while making no change in the driving signals. The output optical signal was received with an optical modulation analyzer (Agilent Technologies, N4391A), combined with a 50-gigasample-per-second (GS/s) storage oscilloscope (Tektronix Inc., DPO72004B), and analyzed offline.

As shown in Fig. 5, clear constellations were obtained for the 20-Gbaud QPSK, 8PSK, 8QAM, and 16QAM signals, which correspond to 80, 120, 120, and 160 Gbit/s, respectively, if we use PDM. The bit-error rates (BERs) for QPSK, 8PSK, and 16QAM were  $<10^{-6}$  (no errors in  $2 \times 10^6$  symbols),  $1.9 \times 10^{-5}$ , and  $3.1 \times 10^{-4}$ , respectively. BER measurement for 8QAM is not currently supported by the analyzer software, but the BER was estimated to be well below  $10^{-4}$  from the measured error-vector magnitude of 9.8%. Optical signal spectra with these four formats are shown in Fig. 6. They almost completely overlap

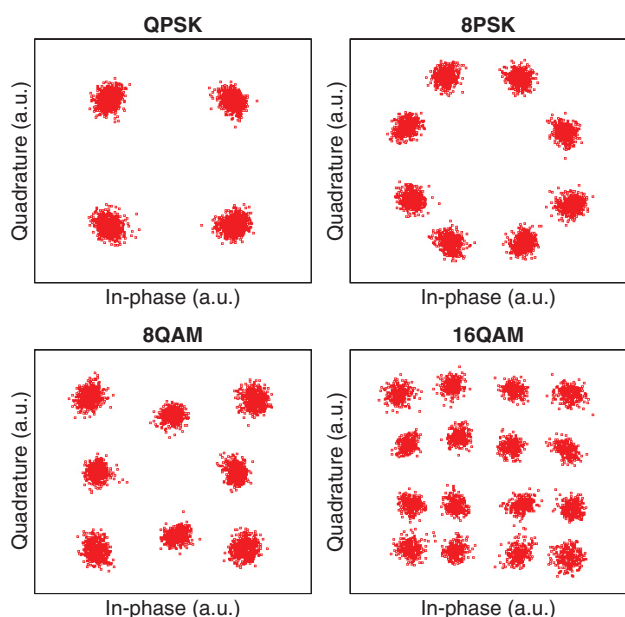


Fig. 5. Constellations of 20-Gbaud QPSK, 8PSK, 8QAM, and 16QAM signals.

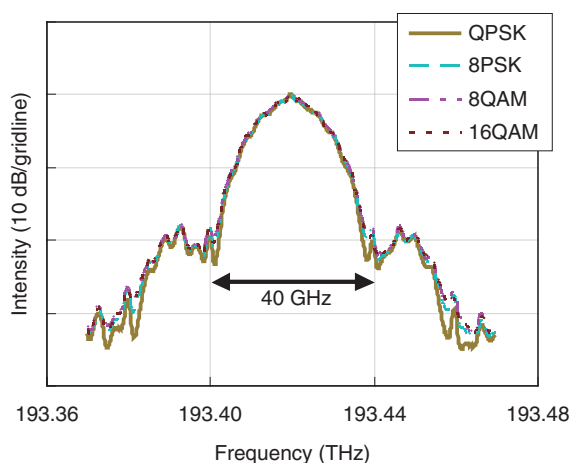


Fig. 6. Optical signal spectra.

and their main-lobe bandwidths are 40 GHz.

### 3. Multicarrier flexible-format modulator

#### 3.1. Design and fabrication

The multicarrier flexible-format modulator was designed to support four-carrier BPSK, two-carrier QPSK, and one-carrier 16-QAM. With a fixed baud rate, all these formats give the same bit rate. By increas-

ing the modulation level and decreasing the number of carriers, we can increase the SE at the cost of reduced receiver sensitivity (transmission distance) [3].

If we were to design separate modulators for the three formats, we would use some straightforward optical-circuit configurations such as those shown in Fig. 7. The four-carrier BPSK modulator consists of three interleave filters (ILFs) for demultiplexing carriers, four MZMs as four BPSK modulators, and three 2×1 couplers. The two-carrier QPSK modulator consists of one ILF, two pairs of MZMs as two QPSK modulators, and one 2×1 coupler. The one-carrier 16-QAM consists of a parallel-quad MZM as a 16-QAM modulator. These modulators have almost the same configuration except for certain passive components, such as the ILFs and couplers.

To provide these three configurations in a common design, we devised a modulator with a novel configuration consisting of three tunable ILFs (TILFs), four MZMs, two 2×1 couplers, and one tunable coupler as shown in Fig. 8(a). To use the modulator as a four-carrier BPSK modulator (four-carrier BPSK mode), TILFs 1–3 are operated normally as carrier-demultiplexers, as shown in Fig. 8(b), and then the tunable coupler is set with a 3-dB coupling ratio. To use the modulator as a two-carrier QPSK modulator (two-carrier QPSK mode), TILFs 2 and 3 are changed so that they operate as 3-dB couplers at the carrier frequency for carrier channels 1 and 2, respectively, to tune the phase condition of the TILFs. For use as a 1-carrier 16-QAM modulator (1-carrier 16-QAM mode), TILFs 1–3 are changed so that they operate as couplers with coupling ratios of two-to-one, 3 dB, and 3 dB, respectively, at the carrier frequency, and then the tunable coupler is set with a two-to-one coupling ratio. Thus, the devised modulator lets us select the modulation format flexibly from among three formats: four-carrier BPSK, two-carrier QPSK, and one-carrier 16-QAM.

The configuration of the fabricated modulator, which generates an optical signal with a total rate of 200 Gbit/s by using eight 25-Gbaud electrical signals in dual polarization operation, is shown in Fig. 9. We used two PLCs (PLC-I and -O) and an X-cut LN chip. The LN chip has an array of sixteen straight phase modulators with eight signal electrodes (coplanar waveguides). PLC-I consists of three TILFs and 1×2 couplers. Each TILF is composed of three Mach-Zehnder interferometers (MZIs) with thermo-optic phase shifters. One MZI is the main TILF, which has two output ports. The others, which have only one output port each, are added to obtain high isolation

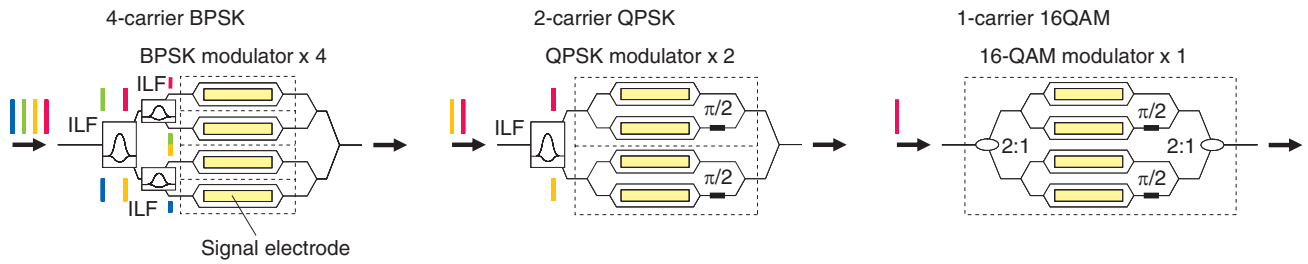


Fig. 7. Optical-circuit diagrams of the four-carrier BPSK, two-carrier QPSK, and one-carrier 16QAM modulators.

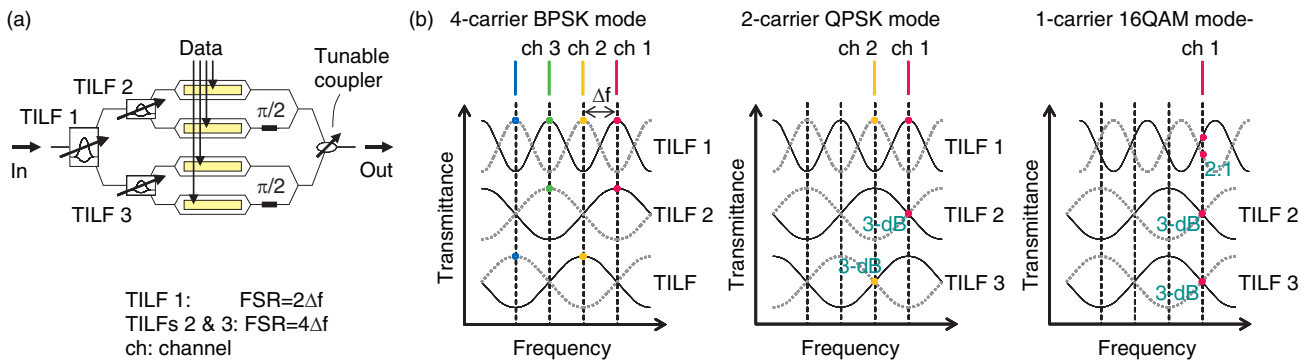


Fig. 8. (a) Optical-circuit diagram of the multicarrier flexible-format modulator. (b) TILF operation for each format mode.

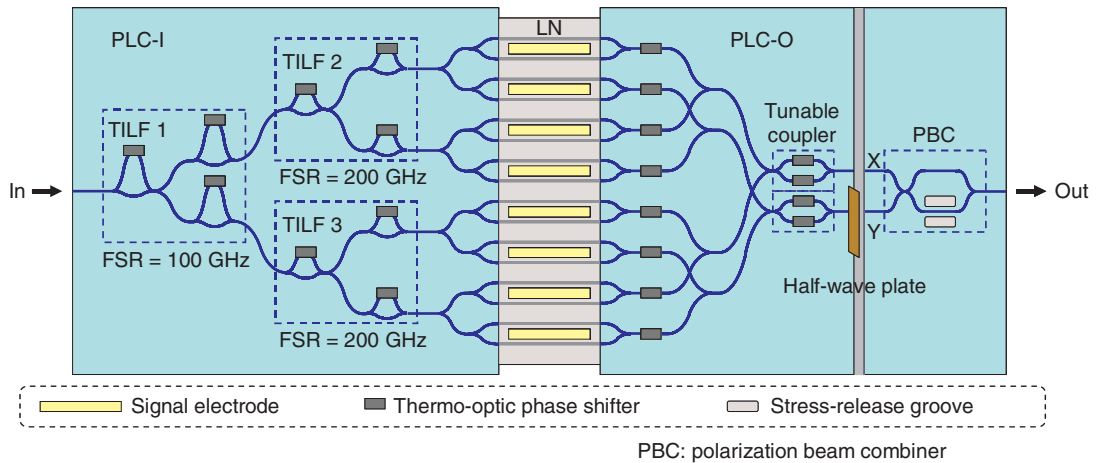


Fig. 9. Configuration of the multicarrier flexible-format modulator.

for demultiplexing. The free spectral range (FSR) of TILF 1 is 100 GHz. TILFs 2 and 3 each have an FSR of 200 GHz. PLC-O consists of 2x1 couplers, thermo-optic phase shifters for IQ (in-phase and quadrature) phase tuning, tunable couplers, a half-wave

plate as a polarization rotator, and a polarization beam combiner. The polarization beam combiner consists of an MZI with stress-release grooves to control waveguide birefringence [14]. We arranged the MZMs in an alternating layout to share the TILFs

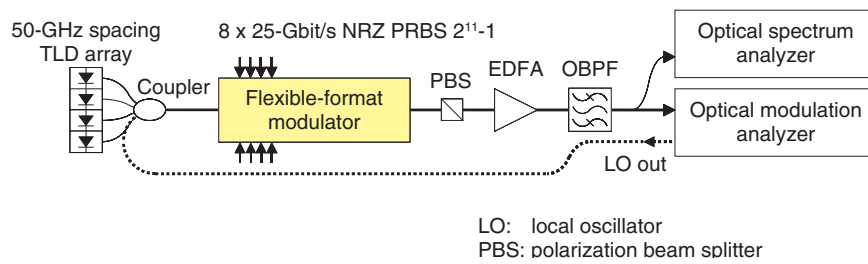


Fig. 10. Experimental setup.

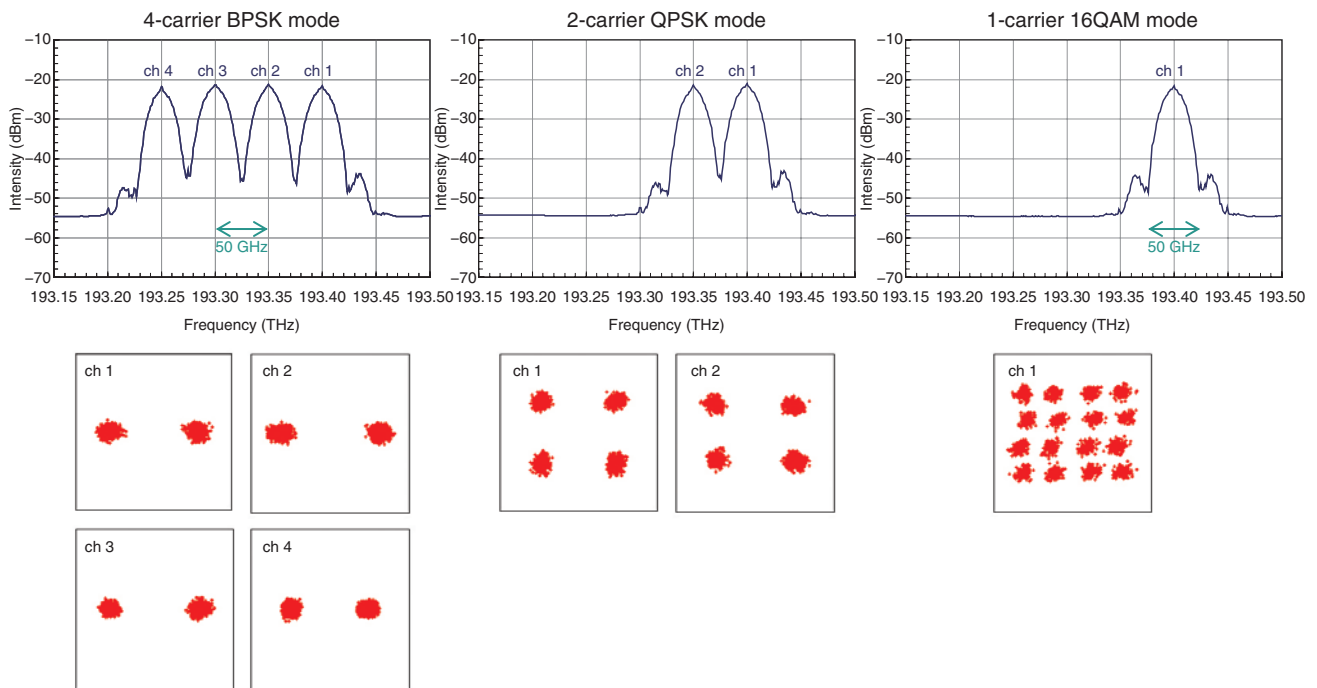


Fig. 11. Measured optical output spectra and constellations of X-polarization signals for 200-Gbit/s operation in four-carrier BPSK, two-carrier QPSK, and one-carrier 16-QAM modes.

for X- and Y-polarizations. We bonded the chips to each other with UV-curable adhesive and then mounted them on an SUS package with radio-frequency connectors. The PLC-I, LN, and PLC-O chips are 33 mm × 13.5 mm, 64 mm × 6.0 mm, and 35 mm × 4.4 mm, respectively, giving a total chip length of 132 mm.

### 3.2. Characteristics

The insertion loss of the modulator was 8.8 dB at a wavelength of 1550 nm when all the thermo-optic phase shifters were tuned so that the transmittance was maximum. The 3-dB bandwidths of the electro-

optic frequency response were around 25 GHz for all the MZMs.

We tested the modulator in the back-to-back self-homodyne setup shown in **Fig. 10**. Four tunable laser diodes (TLDs) with 50-GHz spacing were used as a multicarrier light source. The modulator was driven with eight 25-Gbit/s NRZ  $2^{11}-1$  PRBSs with different delays for 200-Gbit/s operation. We changed the modulation modes by using the TILFs and tunable couplers as described above, while making no change to the driving signals. The number of TLDs constituting the multicarrier source and the TLD wavelengths were changed with the modulation mode. The output

optical signal was received with an optical spectrum analyzer and an optical modulation analyzer, combined with a 50-GS/s storage oscilloscope, and analyzed offline. To enable self-homodyne detection to be used for constellation measurement, the light from the TLD corresponding to the measured carrier channel was changed to that from the local-oscillator in the optical modulation analyzer.

Measured optical output spectra and constellations of X-polarization signals transmitted via a polarization beam splitter are shown in **Fig. 11**. Those for the Y-polarization signals were almost the same. Clear spectra and constellations were obtained in each modulation mode. This means that we were able to select the operating format as four-carrier BPSK, two-carrier QPSK, or one-carrier 16-QAM. The signals with all these formats have the same bit rate of 200 Gbit/s with a symbol rate of 25 Gbaud. Although we used FDM with a frequency spacing twice the baud rate in this first demonstration, we can also readily cover orthogonal frequency division multiplexing (OFDM), in which the frequency spacing equals the baud rate, by changing the FSR of the TILFs.

#### 4. Conclusion

We devised and demonstrated single-carrier and multicarrier flexible-format modulators fabricated with a hybrid configuration of PLCs and LN phase modulators. These modulators let us flexibly select the modulation format simply by using tunable optical circuits while driving the data electrodes with only  $2V\pi$  binary signals. Thanks to the hybrid configuration, the modulators show small optical insertion losses of 7.5 and 8.8 dB, respectively, despite their complicated optical configuration. Flexible-format operations with high baud rates corresponding to bit rates of >100 Gbit/s were successfully demonstrated. These technologies are promising for future optical networks in which various modulation formats will be used flexibly to exploit spectral resources efficiently.

#### References

- [1] A. Sano, H. Masuda, T. Kobayashi, M. Fujiwara, K. Horikoshi, E. Yoshida, Y. Miyamoto, M. Matsui, M. Mizoguchi, H. Yamazaki, Y. Sakamaki, and H. Ishii, "69.1-Tb/s (432 x 171-Gb/s) C- and Extended L-Band Transmission over 240 km Using PDM-16-QAM Modulation and Digital Coherent Detection," Proc. of OFC/NFOEC'10, paper PDPB7, San Diego, CA, USA, 2010.
- [2] Y. Miyamoto and S. Suzuki, "Advanced Optical Modulation and Multiplexing Technologies for High-capacity OTN Based on 100 Gb/s Channel and Beyond," IEEE Commun. Mag., Vol. 48, No. 3, pp. S65–S72, 2010.
- [3] M. Jinno, B. Kozicki, H. Takara, A. Watanabe, Y. Sone, T. Tanaka, and A. Hirano, "Distance-adaptive Spectrum Resource Allocation in Spectrum-sliced Elastic Optical Path Network," IEEE Commun. Mag., Vol. 48, No. 8, pp. 138–145, 2010.
- [4] A. Sano, T. Kobayashi, A. Matsuura, S. Yamamoto, S. Yamanaka, E. Yoshida, Y. Miyamoto, M. Matsui, M. Mizoguchi, and T. Mizuno, "100 x 120-Gb/s PDM 64-QAM Transmission over 160 km Using Linewidth-tolerant Pilotless Digital Coherent Detection," Proc. of ECOC'10, paper PD2.4, Torino, Italy, 2010.
- [5] S. Okamoto, K. Toyoda, T. Omiya, K. Kasai, M. Yoshida, and M. Nakazawa, "512 QAM (54 Gbit/s) Coherent Optical Transmission over 150 km with an Optical Bandwidth of 4.1 GHz," Proc. of ECOC'10, paper PD2.3, Torino, Italy, 2010.
- [6] N. Kikuchi, "Intersymbol Interference (ISI) Suppression Technique for Optical Binary and Multilevel Signal Generation," J. Lightwave Technol., Vol. 25, No. 8, pp. 2060–2068, 2007.
- [7] T. Sakamoto, A. Chiba, and T. Kawanishi, "50-Gb/s 16 QAM by a Quad-parallel Mach-Zehnder Modulator," Proc. of ECOC'07, paper PDS2.8, Berlin, Germany, 2007.
- [8] C. R. Doerr, P. J. Winzer, L. Zhang, L. Buhl, and N. J. Sauer, "Monolithic InP 16-QAM Modulator," Proc. of OFC/NFOEC'08, paper PDP20, San Diego, CA, USA, 2008.
- [9] X. Zhou, J. Yu, M. -F. Huang, Y. Shao, T. Wang, P. Magill, M. Cvijetic, L. Nelson, M. Birk, G. Zhang S. Ten, H. B. Matthew, and S. K. Mishra, "Transmission of 32-Tb/s Capacity over 580 km Using RZ-shaped PDM-8QAM Modulation Format and Cascaded Multimodulus Blind Equalization Algorithm," J. Lightwave Technol., Vol. 28, No. 4, pp. 456–465, 2010.
- [10] H. Yamazaki, T. Yamada, T. Goh, Y. Sakamaki, and A. Kaneko, "64QAM Modulator with a Hybrid Configuration of Silica PLCs and LiNbO<sub>3</sub> Phase Modulators," IEEE Photon. Technol. Lett., Vol. 22, No. 5, pp. 344–346, 2010.
- [11] H. Yamazaki, T. Goh, A. Mori, and S. Mino, "Modulation-level-selectable Optical Modulator with a Hybrid Configuration of Silica PLCs and LiNbO<sub>3</sub> Phase Modulators," Proc. of ECOC'10, paper We.8.E.1, Torino, Italy, 2010.
- [12] T. Goh, H. Yamazaki, T. Kominato, and S. Mino, "Novel Flexible-format Optical Modulator with Selectable Combinations of Carrier Numbers and Modulation Levels Based on Silica-PLC and LiNbO<sub>3</sub> Hybrid Integration," Proc. of OFC/NFOEC'11, paper OWV2, Los Angeles, CA, USA, 2011.
- [13] S. Mino, H. Yamazaki, T. Goh, and T. Yamada, "Multilevel Optical Modulator Utilizing PLC-LiNbO<sub>3</sub> Hybrid-integration Technology," NTT Technical Review, Vol. 9, No. 3, 2011. <https://www.ntt-review.jp/archive/ntttechnical.php?contents=ntr201103fa8.html>
- [14] T. Mizuno, T. Goh, T. Ohya, Y. Hashizume, and A. Kaneko, "Integrated In-band OSNR Monitor Based on Planar Lightwave Circuit," Proc. of ECOC'09, paper 7.2.5, Vienna, Austria, 2009.

**Hiroshi Yamazaki**

Research Engineer, Photonics Integration Laboratory, NTT Photonics Laboratories.

He received the B.S. degree in integrated human studies and the M.S. degree in human and environmental studies from Kyoto University in 2003 and 2005, respectively. In 2005, he joined NTT Photonics Laboratories, where he engaged in research on optical waveguide devices for communication systems. His current research interests include devices and systems for optical transmission using advanced multilevel modulation formats. He is a member of the Institute of Electronics, Information and Communication Engineers (IEICE).

---

**Takashi Goh**

Senior Research Engineer, Photonics Integration Laboratory, NTT Photonics Laboratories.

He received the B.S. and M.S. degrees in electronic and communication engineering from Waseda University, Tokyo, in 1991 and 1993, respectively. In 1993, he joined the NTT Optoelectronics, Ibaraki (now NTT Photonics Laboratories, Kanagawa), where he has been engaged in research on silica-based PLCs including thermo-optic switches, arrayed-waveguide grating multiplexers, multi-degree reconfigurable add-drop multiplexers, and advanced modulators. During 2002–2004, he was engaged in photonic network development such as ROADM ring systems in NTT Innovation Laboratories. He is a member of IEICE and the Japan Society of Applied Physics.

---